

Staggered spin susceptibility and chiral phase transition in thermal QED₃Hong-tao Feng,^{1,3,*} Yu-qing Zhou,¹ Pei-Lin Yin,² and Hong-shi Zong^{2,3,†}¹*Department of Physics, Southeast University, Nanjing 211189, China*²*Department of Physics, Nanjing University, Nanjing 210093, China*³*State Key Laboratory of Theoretical Physics, Institute of Theoretical Physics, CAS, Beijing 100190, China*

(Received 5 August 2013; published 10 December 2013)

Based on the truncated Dyson–Schwinger equation, we first study the influence of the vertex correction on the staggered spin susceptibility χ^s . The numerical results show that the vertex correction plays an important role in the study of the staggered spin susceptibility. We then generalize the above work to the case of finite temperature. It is found for the first time that, as the temperature increases, the chiral condensate vanishes at the phase transition point where χ^s reveals an obvious skip, and therefore as a physical observable, the staggered spin susceptibility could be regarded as the order parameter of chiral phase transition in QED₃.

DOI: 10.1103/PhysRevD.88.125022

PACS numbers: 11.10.Kk, 11.15.Tk, 11.30.Qc

I. INTRODUCTION

Quantum electrodynamics in $(2 + 1)$ dimensions (QED₃) is a well-studied field-theoretical model. This Abelian system exhibits several interesting features, similar to QCD, for instance, dynamical chiral symmetry breaking (DCSB) [1–15] and confinement [16–18]. Moreover, it is super-renormalizable so that it is not plagued with ultraviolet divergences. Thus, QED₃ is an ideal model to study nonperturbative phenomena. Although some discussion concerning the origins of confinement and DCSB in QED₃ is needed, the mechanism of confinement and DCSB of QED₃ is quite different from that in QCD. Nevertheless, it is generally believed that QED₃ provides a very useful playground within which to identify unambiguous signals of these phenomena. The fact that the theory exists in three dimensions obscures nothing of the essence of these fundamentally important questions.

In addition, QED₃ can be applied in condensed matter physics to unpuzzle some realistic microscopic mechanisms. Especially, since the discovery of the high- T_c superconductivity, QED₃ has attracted more attention. It is generally believed that QED₃ with N flavors can be regarded as a possible effective theory for high- T_c superconductivity in underdoped cuprates [19–21] and graphene [22–24]. Because of these features, QED₃ has been extensively studied in recent years.

A breakthrough in the research of chiral phase transition (CPT) in QED₃ was achieved in a paper of Appelquist *et al.* [3], who found that CPT happens when the number of flavors of a massless fermion reaches a critical number $N_c \approx 3.24$. They arrived at this conclusion by analytically and numerically solving the Dyson–Schwinger equation (DSE) for the fermion self-energy. Later, some groups

adopted improved schemes for the DSE and obtained qualitatively similar results [25–27]. It is generally believed that as the temperature increases the original chiral symmetry broken phase undergoes CPT into a chiral symmetric phase at a critical temperature T_c . Recently, based on the truncated DSE for the fermion propagator in QED₃, it was found that the fermion number susceptibility shows a continuous behavior at high temperature, which exhibits a typical characteristic of the second-order phase transition around T_c [28]. Moreover, the entropy shows a continuous behavior, while the specific heat jumps at the critical temperature, which indicates that the above susceptibilities are suitable for investigating the characteristic of chiral phase transition at finite temperature [29].

Because of its crucial role in the pseudogap phase in effective QED₃ theory of the insulating parent compound of the copper oxide superconductors, the staggered spin susceptibility (χ^s) is widely studied in condensate matter physics [30–32]. Since this physical observable contains some basic correlative properties of the system and, especially, since it can be easily measured, it provides an ideal tool to learn the characteristics of those strongly correlated systems [33–35]. In a recent work [36], based on functional analysis, the general expression for the susceptibility was obtained, and so the value of χ^s can be obtained via the truncated DSE for fermion and boson propagators. However, in this work, the vertex correction for χ^s is ignored. One motivation of this work is to investigate the influence of the vertex correction on the staggered spin susceptibility. Another motivation of this work is to generalize the study in Ref. [36] to the case of finite temperature and investigate the influence of the temperature effect on the staggered spin susceptibility. Just as mentioned above, the staggered spin susceptibility reflects some basic correlative properties of the system. It is interesting to study the behavior of the staggered spin susceptibility at the chiral phase transition point.

*fenght@seu.edu.cn

†zonghs@chenwang.nju.edu.cn

In this paper, we shall adopt the truncated DSE to investigate the staggered spin susceptibility and the chiral condensate and try to say something about the relation between the staggered spin susceptibility and chiral phase transition in thermal QED₃.

II. FORMALISM OF STAGGERED SPIN SUSCEPTIBILITY

In Euclidean space, the Lagrangian of QED₃ with N fermion flavors in the chiral limit reads

$$\mathcal{L} = \sum_{j=1}^N \bar{\psi}_j (\partial / + ieA /) \psi_j + \frac{1}{4} F_{\sigma\nu}^2, \quad (1)$$

where the four-component spinors are employed. At zero temperature and density, this Lagrangian is chiral symmetric, but DCSB occurs because of nonperturbative effects. The order parameter of CPT is defined by

$$\langle \bar{\psi} \psi \rangle = \text{Tr}[S(x \equiv 0)] = \int \frac{d^3 p}{(2\pi)^3} \frac{4B(p^2)}{G(p^2)}, \quad (2)$$

with $G(p^2) = A^2(p^2)p^2 + B^2(p^2)$. The two functions $A(p^2)$ and $B(p^2)$ in the above equation are related to the inverse fermion propagator

$$S^{-1}(p) = i\gamma \cdot p A(p^2) + B(p^2). \quad (3)$$

To obtain the fermion propagator and also the fermion chiral condensate, it is theoretically valuable to give a general recipe for calculating this function in the framework of the truncated DSE approach,

$$S^{-1}(p) = i\gamma \cdot p + \alpha \int \frac{d^3 k}{(2\pi)^3} \gamma_\sigma S(k) \gamma_\nu D_{\sigma\nu}(q), \quad (4)$$

with $q = p - k$. The coupling constant $\alpha = e^2$ has dimension 1 and provides us with a mass scale. For simplicity, in this paper, the momentum, temperature, and fermion self-energy are all measured in units of α ; namely, we choose a kind of natural unit in which $\alpha = 1$.

The general expression for the low-energy behavior of the regularized staggered spin susceptibility was given by Ref. [36],

$$\begin{aligned} \chi^s &= \langle S^z(0) S^z(0) \rangle \\ &= \int \frac{d^3 p}{(2\pi)^3} \text{Tr}[S(p) \Gamma(p) S(p) - S_0(p) \mathbf{1} S_0(p)] \\ &= 4 \int \frac{d^3 p}{(2\pi)^3} \left[\frac{F(p^2)}{G(p^2)} - \frac{1}{p^2} \right], \end{aligned} \quad (5)$$

where Lorentz structure analysis gives $\Gamma(p) = i\gamma_5 \gamma \cdot p H(p^2) + \gamma_5 F(p^2)$ and

$$F(p^2) = 1 + 2 \int \frac{d^3 k}{(2\pi)^3} \frac{F(k^2)}{G(k^2)[q^2 + \Pi(q^2)]}. \quad (6)$$

The next task is to calculate $A(p^2)$, $B(p^2)$, and $F(p^2)$. From Eqs. (3) and (4), we obtain the equation satisfied by $A(p^2)$ and $B(p^2)$,

$$A(p^2) = 1 - \frac{1}{4p^2} \int \frac{d^3 k}{(2\pi)^3} \text{Tr}[i(\gamma p) \gamma_\sigma S(k) \gamma_\nu D_{\sigma\nu}(q)], \quad (7)$$

$$B(p^2) = \frac{1}{4} \int \frac{d^3 k}{(2\pi)^3} \text{Tr}[\gamma_\sigma S(k) \gamma_\nu D_{\sigma\nu}(q)]. \quad (8)$$

Another involved function $D_{\sigma\nu}(q)$ is the full gauge boson propagator, which in the Landau gauge can be written as

$$D_{\sigma\nu}(q) = \frac{\delta_{\sigma\nu} - q_\sigma q_\nu / q^2}{q^2 + \Pi(q^2)}, \quad (9)$$

where $\Pi(q^2)$ is the vacuum polarization for the gauge boson, which is satisfied by the polarization tensor

$$\Pi_{\sigma\nu}(q^2) = -N \int \frac{d^3 k}{(2\pi)^3} \text{Tr}[S(k) \gamma_\sigma S(q+k) \gamma_\nu]. \quad (10)$$

Using the relation between the vacuum polarization $\Pi(q^2)$ and $\Pi_{\sigma\nu}(q^2)$,

$$\Pi_{\sigma\nu}(q^2) = \left(\delta_{\sigma\nu} - \frac{q_\sigma q_\nu}{q^2} \right) \Pi(q^2), \quad (11)$$

we can obtain an equation for $\Pi(q^2)$ that has an ultraviolet divergence. Fortunately, it is present only in the longitudinal part and is proportional to $\delta_{\sigma\nu}$. This divergence can be removed by the projection operator

$$\mathcal{P}_{\sigma\nu} = \delta_{\sigma\nu} - 3 \frac{q_\sigma q_\nu}{q^2}, \quad (12)$$

and then we obtain a finite vacuum polarization [17]. Finally, the three coupled functions $A(p^2)$, $B(p^2)$, and $\Pi(q^2)$ associated with the DSE of the fermion propagator reduce

$$A(p^2) = 1 + \int \frac{d^3 k}{(2\pi)^3} \frac{2A(k^2)(pq)(kq)/q^2}{p^2 G(k^2)[q^2 + \Pi(q^2)]}, \quad (13)$$

$$B(p^2) = \int \frac{d^3 k}{(2\pi)^3} \frac{2B(k^2)}{G(k^2)[q^2 + \Pi(q^2)]}, \quad (14)$$

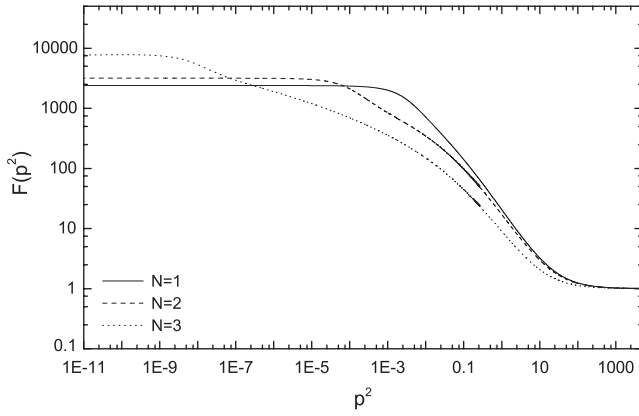


FIG. 1. The typical behaviors of the vertex function of the susceptibility with several N .

$$\Pi(q^2) = N \int \frac{d^3k}{(2\pi)^3} \frac{2A(k^2)A(p^2)}{G(k^2)G(p^2)} \times [2k^2 - 4(k \cdot q) - 6(k \cdot q)^2/q^2]. \quad (15)$$

By application of iterative methods for the truncated DSE of the fermion propagator in Eqs. (13–15) and (6), we can obtain A , B , Π , and F . The typical behavior of the vertex function $F(p^2)$ is shown in Fig. 1. From Fig. 1, it is seen that the vertex function decreases and tends to 1 in the large momentum limit (this results in what one expects in advance; this is because in the large momentum limit the dressed vertex should approach the corresponding bare vertex), while it reduces to a constant in the low-energy region and the infrared value increases with the rise of N .

Then, substituting the obtained fermion propagator and the vertex function into Eq. (5), we obtain the susceptibility with several N , and they are plotted in Fig. 2. To give an insight of the effect of vertex function $F(p^2)$, in Fig. 2 we also illustrate the susceptibility (χ_b^s) under a bare vertex approximation, which is obtained by putting $F(p^2) = 1$ into Eq. (5). One sees that χ^s is apparently larger than χ_b^s for any N . Moreover, χ^s decreases with the rise of N , while χ_b^s increases. This result indicates that the vertex

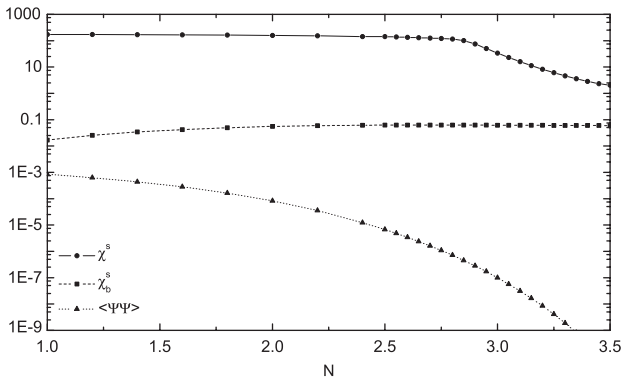


FIG. 2. The value of the susceptibility obtained using bare vertex approximation and the improved vertex in Nambu phase.

function $F(p^2)$ must be taken into account when one calculates the staggered spin susceptibility.

III. SUSCEPTIBILITY AT FINITE TEMPERATURE

Apart from zero temperature, the $O(3)$ symmetry of the system reduces to $O(2)$, and the fermion propagator can be written as

$$S^{-1}(T, P) = i\vec{\gamma} \cdot \vec{P} A_{\parallel}(P^2) + i\varpi_n \gamma_3 A_3(P^2) + B(P^2), \quad (16)$$

where $\varpi_n = (2n + 1)\pi T$. As a general discussion, we only investigate the spin susceptibility in the case of $N = 1$. Adopting the DSE for the fermion propagator and techniques of the temperature field theory, we can resolve the above three unknown functions to analyze the chiral transitions of QED₃ at finite temperature. Nevertheless, following the lowest-order DSE for the fermion propagator, Dorey investigated the DCSB of QED₃ and showed that QED₃ at $N = 1$ undergoes CPT into a chiral symmetric phase when the temperature reaches a critical value T_c . Later, the authors of Refs. [37,38] adopted an improved truncated scheme for the DSE to study the CPT and found that the correctional contribution to the factor only slightly changes the results qualitatively. These conclusions suggest that the lowest-order DSE for the fermion propagator is a suitable approximation for studying CPT in thermal QED₃.

To obtain a qualitative picture of the susceptibility, we employ a familiar framework to obtain the scalar part of the inverse fermion propagator for which the zero frequency approximation of boson polarization is widely adopted [37–39]. In addition, the conclusions in Ref. [40] illustrated that, by summing over the frequency modes and taking suitable simplifications, the qualitative aspects of the result obtained under the zero-frequency approximation for the wave-function renormalization A and the fermion mass function B do not undergo significant changes. From this, we also ignore the frequency dependence of fermion self-energy, and then the corresponding DSE for the scalar part of inverse fermion propagator reads [38]

$$\begin{aligned} B(P^2) &= 2 \int \frac{d^2K}{(2\pi)^2} \sum_n \frac{B(K^2) [Q^2 + \Pi(Q)]}{\varpi_n^2 + K^2 + B^2(K^2)} \\ &= \int \frac{d^2K}{(2\pi)^2} \frac{B(K^2) \tanh \frac{\mathcal{E}_k}{2T}}{\mathcal{E}_k [Q^2 + \Pi(Q)]}, \end{aligned} \quad (17)$$

where $Q = P - K$, $\mathcal{E}_k = \sqrt{K^2 + B^2(K^2)}$, and $\Pi(Q)$ denotes the boson polarization in the chiral limit[41,28],

$$\begin{aligned}\Pi(Q) &= \frac{T}{\pi} \int_0^1 dx \ln \left[4 \cosh^2 \frac{\sqrt{x(1-x)}Q^2}{2T} \right] \\ &\approx \frac{Q}{8} + T \frac{2 \ln 2}{\pi} \exp \left(-\frac{\pi Q}{16T \ln 2} \right).\end{aligned}\quad (18)$$

Here, the identity

$$\sum_n \frac{1}{\omega_n^2 + x^2} = \frac{1}{2} \frac{\tanh \frac{x}{2T}}{x} \quad (19)$$

is used. By the same way, the renormalized susceptibility (5) at finite temperature in the framework of the lowest-order approximation of the DSE reduces to

$$\begin{aligned}\chi^s(T, \mu) &= 4T \sum_n \int \frac{d^2 P}{(2\pi)^2} \left[\frac{F(P^2)}{\omega_n^2 + \mathcal{E}_p^2} - \frac{1}{\omega_n^2 + P^2} \right] \\ &= 2 \int \frac{d^2 P}{(2\pi)^2} \left[\frac{F(P^2) \tanh \frac{\mathcal{E}_p}{2T}}{\mathcal{E}_p} - \frac{\tanh \frac{\sqrt{P^2}}{2T}}{\sqrt{P^2}} \right],\end{aligned}\quad (20)$$

and the corresponding vertex function F is written as

$$\begin{aligned}F(P^2) &= 1 + 2T \sum_n \int \frac{d^2 K}{(2\pi)^2} \frac{F(K^2) / [Q^2 + \Pi(Q)]}{\omega_n^2 + K^2 + B^2(K^2)} \\ &= 1 + \int \frac{d^2 K}{(2\pi)^2} \frac{F(K^2) \tanh \frac{\mathcal{E}_k}{2T}}{\mathcal{E}_k [Q^2 + \Pi(Q)]}.\end{aligned}\quad (21)$$

It can be easily seen that the above fermion self-energy and vertex functions reduce to the case of lowest-order approximation for Eqs. (14) and (6) at $T \rightarrow 0$. Then, from the above equations (17–21), we can obtain the susceptibility and chiral fermion condensate at finite T and try to say something about the staggered spin susceptibility around the critical point of the CPT.

IV. NUMERICAL RESULTS

By solving the DSE for the fermion propagator using the numerical iteration method, we can obtain the fermion self-energy function $B(P^2)$. From it, we can calculate the vertex function, and its typical behaviors can be seen in Fig. 3. For any value of temperature, the vertex function is almost constant in the infrared region, while it falls with the increasing momentum and reduces to 1 in the high-energy limit. From the infrared value of $F(P^2)$, it is seen that with increasing temperature, its infrared value falls slowly in the low- and high-temperature region but falls rapidly near $T = 2.5 \times 10^{-2}$.

Finally, based on the fermion self-energy and the vertex function, we immediately obtain the fermion chiral condensate and the staggered spin susceptibility with a range of temperature, and the results are plotted in Fig. 4. The upper line of Fig. 4 gives the behavior of staggered spin susceptibility, while the lower line in this figure shows the

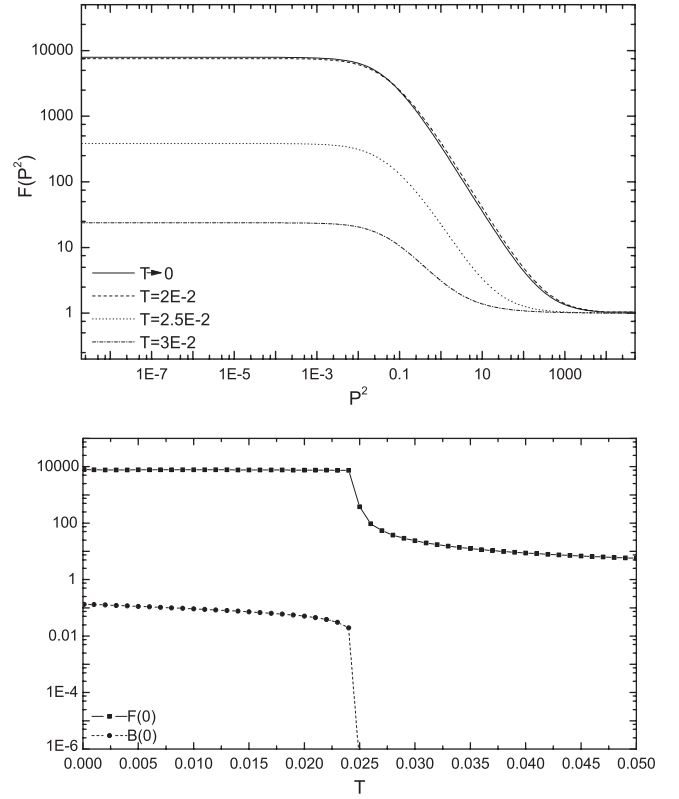


FIG. 3. The typical behaviors of $F(P^2)$ (top) and the infrared value of $F(P^2)$ and $B(P^2)$ (bottom) with a range of T .

behavior of the fermion chiral condensate. As can be seen in Fig. 4, χ^s almost keeps a constant at small temperature (where, in fact, the susceptibility increases tardily with the rise of T), while it shows an apparent skip at some critical temperature. From Fig. 4, it can also be seen that the fermion chiral condensate decreases as the temperature rises and vanishes at the critical point $T_c \approx 2.5 \times 10^{-2}$ where the CPT occurs. Comparing these two lines, it is found that the point of skip for the staggered spin susceptibility corresponds to T_c . This could be regarded as a prediction

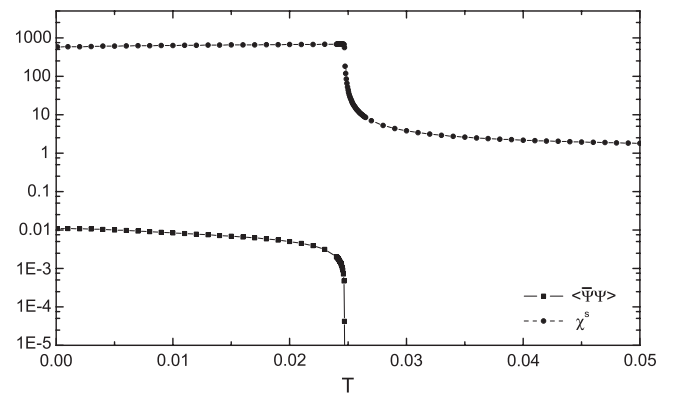


FIG. 4. The temperature dependence of $\langle \bar{\psi} \psi \rangle$ and χ^s .

of our study. Here, it should be noted that the fermion chiral condensate is not a physical observable, whereas the staggered spin susceptibility is. Therefore, it is more reasonable to regard the staggered spin susceptibility as the order parameter for chiral phase transition in QED₃.

V. CONCLUSIONS

In this paper, based on the suitable truncated Dyson–Schwinger equation, we aim to analyze the staggered spin susceptibility at finite temperature to give an insight for the relation between the susceptibility and chiral phase transition. We first study the staggered spin susceptibility in QED₃ by including the correction of the vertex function. Our numerical results show that the calculated value of the staggered spin susceptibility is apparently different from that obtained using bare vertex approximation, and hence the vertex correction plays an important role in the study of staggered spin susceptibility. Then, we generalize this study to the case of finite temperature and find that the staggered spin susceptibility shows an apparent skip at a temperature corresponding to the critical point of the chiral phase transition. The appearance of the skip of staggered spin

susceptibility at the critical temperature for chiral phase transition suggests that the staggered spin susceptibility can be regarded as the order parameter of chiral phase transition in QED₃ and could be competent to study the chiral phase transition in strongly correlated condensed matter physics.

Just as mentioned in Refs. [42,43], the lowest-order DSE for the fermion propagator and the zero-frequency approximation adopted in the present work are inaccurate. To further confirm the conclusion obtained in our work, we need to go beyond the lowest-order DSE and the zero-frequency approximation to study this problem in the future.

ACKNOWLEDGMENTS

We would like to thank Yu Jiang and Qiang-hua Wang for their helpful discussions. This work was supported by the National Natural Science Foundation of China (under Grants No. 11047005, No. 11105029, No. 11275097, No. 10935001, and No. 11075075) and the Research Fund for the Doctoral Program of Higher Education (under Grant No. 2012009111002).

-
- [1] R. D. Pisarski, *Phys. Rev. D* **29**, 2423 (1984).
 - [2] T. W. Appelquist, M. Bowick, D. Karabali, and L. C. R. Wijewardhana, *Phys. Rev. D* **33**, 3704 (1986).
 - [3] T. Appelquist, D. Nash, and L. C. R. Wijewardhana, *Phys. Rev. Lett.* **60**, 2575 (1988).
 - [4] D. Nash, *Phys. Rev. Lett.* **62**, 3024 (1989).
 - [5] M. R. Pennington and D. Walsh, *Phys. Lett. B* **253**, 246 (1991).
 - [6] D. C. Curtis, M. R. Pennington, and D. Walsh, *Phys. Lett. B* **295**, 313 (1992).
 - [7] C. J. Burden and C. D. Roberts, *Phys. Rev. D* **44**, 540 (1991).
 - [8] K.-I. Kondo and H. Nakatani, *Prog. Theor. Phys.* **87**, 193 (1992).
 - [9] A. Bashir, *Phys. Lett. B* **491**, 280 (2000).
 - [10] A. Bashir, A. Huet, and A. Raya, *Phys. Rev. D* **66**, 025029 (2002).
 - [11] G. Z. Liu and G. Cheng, *Phys. Rev. D* **67**, 065010 (2003).
 - [12] H. T. Feng, F. Hu, W. M. Sun, and H. S. Zong, *Commun. Theor. Phys.* **43**, 501 (2005).
 - [13] H. T. Feng, W. M. Sun, F. Hu, and H. S. Zong, *Int. J. Mod. Phys. A* **20**, 2753 (2005).
 - [14] A. Bashir, A. Raya, I. C. Cloët, and C. D. Roberts, *Phys. Rev. C* **78**, 055201 (2008).
 - [15] P. M. Lo and E. S. Swanson, *Phys. Rev. D* **83**, 065006 (2011).
 - [16] M. Göpfert and G. Mack, *Commun. Math. Phys.* **82**, 545 (1982).
 - [17] N. Brown and M. R. Pennington, *Phys. Rev. D* **39**, 2723 (1989).
 - [18] P. Maris, *Phys. Rev. D* **52**, 6087 (1995).
 - [19] I. F. Herbut and B. H. Seradjeh, *Phys. Rev. Lett.* **91**, 171601 (2003).
 - [20] M. Franz, Z. Tesanovic, and O. Vafek, *Phys. Rev. B* **66**, 054535 (2002).
 - [21] G. Z. Liu, *Phys. Rev. B* **71**, 172501 (2005) and references therein.
 - [22] K. S. Novoselov, A. K. Geim, S. V. Morozov, D. Jiang, M. I. Katsnelson, I. V. Grigorieva, S. V. Dubonos, and A. A. Firsov, *Nature (London)* **438**, 197 (2005).
 - [23] V. P. Gusynin, S. G. Sharapov, and J. P. Carbotte, *Int. J. Mod. Phys. B* **21**, 4611 (2007).
 - [24] C. X. Zhang, G. Z. Liu, and M. Q. Huang, *Phys. Rev. B* **83**, 115438 (2011).
 - [25] P. Maris, *Phys. Rev. D* **54**, 4049 (1996).
 - [26] V. Gusynin, A. Hams, and M. Reenders, *Phys. Rev. D* **63**, 045025 (2001).
 - [27] C. S. Fischer, R. Alkofer, T. Dahm, and P. Maris, *Phys. Rev. D* **70**, 073007 (2004).
 - [28] H. T. Feng, S. Shi, P. L. Yin, and H. S. Zong, *Phys. Rev. D* **86**, 065002 (2012).
 - [29] H. T. Feng, B. Wang, W. M. Sun, and H. S. Zong, *Phys. Rev. D* **86**, 105042 (2012).
 - [30] D. H. Kim and P. A. Lee, *Ann. Phys. (N.Y.)* **272**, 130 (1999).
 - [31] M. Franz, D. E. Sheehy, and Z. Tesanovic, *Phys. Rev. Lett.* **88**, 257005 (2002).
 - [32] E. Demler, W. Hanke, and S. C. Zhang, *Rev. Mod. Phys.* **76**, 909 (2004).

- [33] A. V. Chubukov, S. Sachdev, and J. W. Ye, *Phys. Rev. B* **49**, 11919 (1994).
- [34] P. E. Engelstad and K. Yamada, *Phys. Rev. B* **52**, 13029 (1995).
- [35] W. Rantner and X. G. Wen, *Phys. Rev. B* **66**, 144501 (2002) and references therein.
- [36] J. F. Li, H. T. Feng, Y. Jiang, W. M. Sun, and H. S. Zong, *Phys. Rev. D* **87**, 116008 (2013).
- [37] I. J. R. Aitchison, N. Dorey, M. Klein-Kreisler, and N. E. Mavromatos, *Phys. Lett. B* **294**, 91 (1992).
- [38] N. Dorey and N. E. Mavromatos, *Phys. Lett. B* **266**, 163 (1991).
- [39] N. Dorey and N. E. Mavromatos, *Nucl. Phys.* **B386**, 614 (1992).
- [40] A. Ayala and A. Bashir, *Phys. Rev. D* **67**, 076005 (2003).
- [41] I. J. R. Aitchison and M. Klein-Kreisler, *Phys. Rev. D* **50**, 1068 (1994).
- [42] P. M. Lo and E. S. Swanson, *Phys. Lett. B* **697**, 164 (2011).
- [43] P. M. Lo and E. S. Swanson, arXiv:1307.5834.